Available online at www.sciencedirect.com

ScienceDirect

Physics Procedia 74 (2015) 183 – 190

Physics Procedia

Conference of Fundamental Research and Particle Physics, 18-20 February 2015, Moscow, Russian Federation

Physical performance of GAMMA-400 telescope. Angular resolution, proton and electron separation

A.A. Leonov[a,*], A.M. Galper[a,b], I.V. Arkhangelskaja[a], A.I. Arkhangelskiy[a], Y.V. Gusakov[b], V.V. Kadilin[a], M.D. Kheymits[a], V.V. Mikhailov[a], P.Y. Naumov[a], M.F. Runtso[a], S.I. Suchkov[b], N.P. Topchiev[b], Y.T. Yurkin[a], V.G. Zverev[a]

[a]*National Research Nuclear University MEPhI (Moscow Engineering Physics Institute), Kashirskoe highway 31, Moscow 115409, Russia*
[b] *Lebedev Physical Institute, Russian Academy of Sciences, Leninskiy prospekt 53, Moscow, 119991, Russia*

Abstract

The specially designed GAMMA-400 gamma-ray telescope will realize the measurements of gamma-ray fluxes and cosmic-ray electrons and positrons in the energy range from 100 MeV to several TeV. Such measurements concern with the following broad range of scientific topics. Search for signatures of dark matter, investigation of gamma-ray point and extended sources, studies of the energy spectra of Galactic and extragalactic diffuse emission, studies of gamma-ray bursts and gamma-ray emission from the active Sun, as well as high-precision measurements of spectra of high-energy electrons and positrons, protons, and nuclei up to the knee. To clarify these scientific problems with the new experimental data the GAMMA-400 gamma-ray telescope possesses unique physical characteristics comparing with previous and present experiments. For gamma-ray energies more than 100 GeV GAMMA-400 provides the energy resolution ~1% and angular resolution better than 0.02 deg. The methods, developed to reconstruct the direction of incident gamma photon, are presented in this paper, as well as, the capability of the GAMMA-400 gamma-ray telescope to distinguish electrons and positrons from protons in cosmic rays is discussed.

Peer-review under responsibility of the National Research Nuclear University MEPhI (Moscow Engineering Physics Institute)

Keywords: gamma-ray telescope; hadron and electromagnetic showers; gamma rays; cosmic rays; space experiments

1. Introduction

The GAMMA-400 instrument has developed to address a broad range of scientific goals, such as search for signatures of dark matter, studies of Galactic and extragalactic gamma-ray sources, Galactic and extragalactic

* Corresponding author. Tel.: +7-917-541-57-44.
E-mail address: alexeyanatolievich@rambler.ru

Peer-review under responsibility of the National Research Nuclear University MEPhI (Moscow Engineering Physics Institute)
doi:10.1016/j.phpro.2015.09.185

diffuse emission, gamma-ray bursts, as well as high-precision measurements of spectra of cosmic-ray electrons, positrons, and nuclei [1]. In this paper, the method, developed to reconstruct the direction of incident gamma photon, and the methods to separate electrons and protons in the GAMMA-400 gamma-ray telescope is presented. gamma-ray telescope; hadron and electromagnetic showers; gamma rays; cosmic rays; space experiments

The detector systems used in the satellite-borne experiments and devoted to study high-energy cosmic rays have a possibility not only to measure energies, but also to identify protons and electrons. This identification is usually based on a comparison of longitudinal and transversal shower profiles and the total energy deposition in a calorimeter system taking into account that electromagnetic and hadronic showers have different spatial and energy topology form [2]. Moreover, the number of neutrons generated in the electromagnetic cascade is much less than that in the hadronic cascade. The neutron detection essentially improves separation of electrons from protons [3, 4].

The combined information from all detector systems provides the rejection factor for vertical and inclined protons better than 10^5.

2. The GAMMA-400 gamma-ray telescope

The GAMMA-400 physical scheme is shown in Fig. 1. GAMMA-400 consists of scintillation anticoincidence top and lateral detectors (AC top and AC lat), converter-tracker (C) with 13 layers of double (x, y) silicon strip coordinate detectors with pitch of 0.08 mm (the first three and final one layers are without tungsten while the middle nine layers are interleaved with nine tungsten conversion foils), scintillation detectors (S1 and S2) of time-of-flight system (TOF), calorimeter from two parts (CC1 and CC2), lateral detectors (LD), scintillation detectors (S3 and S4) and neutron detector (ND) to separate hadronic and electromagnetic showers. The anticoincidence detectors surrounding the converter-tracker are served to distinguish gamma-ray events from the much more numerous charged-particle events. Converter-tracker information is applied to precisely determine the direction of each incident particle and calorimeter measurements are used to determine its energy. All scintillation detectors consist from two independent layers. Each layer has thickness of 1 cm. The time-of-flight system, where detectors S1 and S2 are separated by 500 mm, determines the top-down direction of arriving particle. Additional scintillation detectors S3 and S4 improve hadronic and electromagnetic showers separation.

The imaging calorimeter CC1 consists of 2 layers of double (x, y) silicon strip coordinate detectors (pitch of 0.1 mm) interleaved with planes from CsI(Tl) crystals, and the electromagnetic calorimeter CC2 consists of CsI(Tl) crystals. The total converter-tracker thickness is about 1 X_0 (X_0 is the radiation length). The thicknesses of CC1 and CC2 are 2 X_0 and 23 X_0, respectively. The total calorimeter thickness is 25 X_0 or 1.2 λ_0 (λ_0 is nuclear interaction length). Using thick calorimeter allows us to extend the energy range up to several TeV and to reach the energy resolution better than 1% above 100 GeV.

The signals from AC detectors used for charged particles and gamma rays identification due specially designed for GAMMA-400 methods of backsplash rejection.

3. The method to reconstruct the incident direction of high-energy gamma in the GAMMA-400 gamma-ray space telescope during ground data processing

Converter-tracker consists of 13 layers of silicon-strip detectors, 9 of which being interleaved with 9 tungsten foils. The first foil with thickness 0.2 X_0 (where X_0 is the radiation length) located after third upper strip detectors layer, other nine ones with thickness 0.1 X_0 positioned after following strip detectors layer each. Correspondingly first three and last one strip layers are without preceded tungsten conversion foils. Every converter-tracker strip detectors layer being composed of two plates of mutually perpendicular strips (X and Y) with pitch of 0.08 mm. Photons are converted into electron–positron pairs in the tungsten conversion foils inside converter–tracker. The method to reconstruct the incident gamma-quanta direction was developed with the GEANT4 simulation toolkit software [5]. The reconstruction procedure applies the energy deposition in 12 silicon-strip layers located below the first conversion foil. Ten of them compose the converter-tracker, whereas other 2 ones being located in imaging calorimeter CC1.

A direction-reconstruction technique based on strip energy release has been developed. The plane flux of gamma has simulated just above top AC plane. At first, for each silicon-strip layer with energy release the following

procedure is applied. The distribution of the sum of energy releases in strips along strip positions is constructed (Fig. 2a). The horizontal line is median, which is calculated as a half sum of the extreme points for constructed distribution. The intersection point of median with piecewise continuous distribution gives the estimation of median energy location in silicon-strip layer (Fig. 2a).

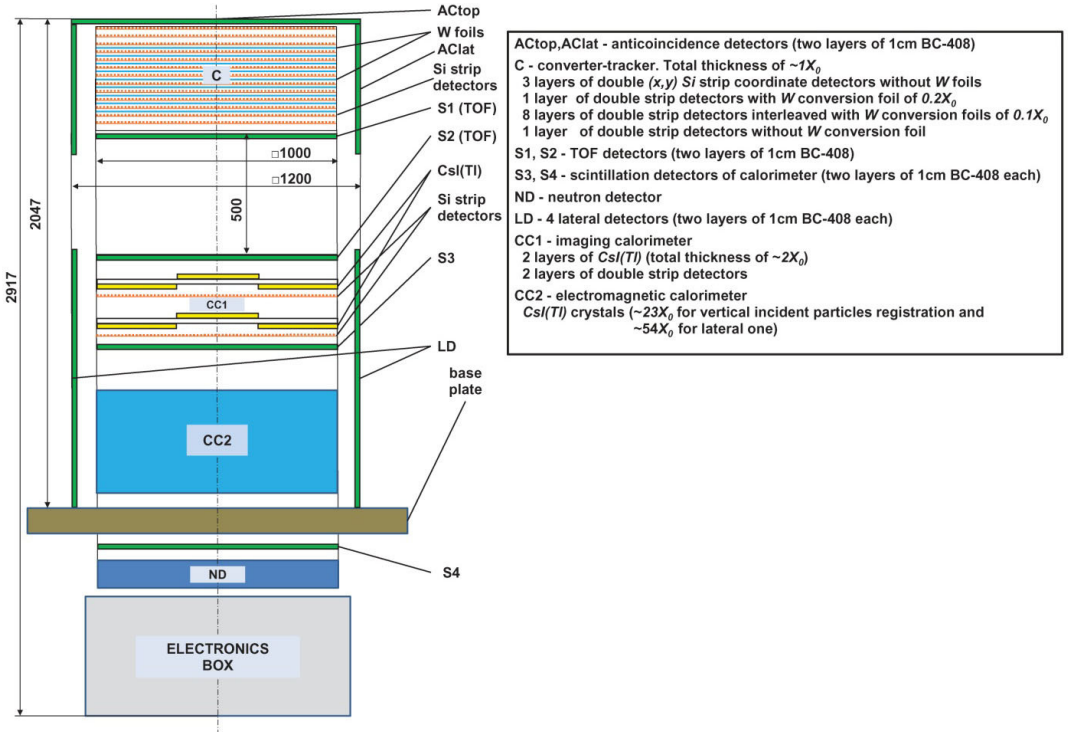

Fig. 1. The GAMMA-400 physical scheme. AC top is the top anticoincidence detector, AC lat are lateral anticoincidence detectors, C is the converter-tracker; S1 (ToF) and S2 (ToF) are scintillation detectors of the time-of-flight system, CC1 and CC2 are coordinate-sensitive and electromagnetic calorimeter, S3 and S4 are scintillation detectors, ND is the neutron detector.

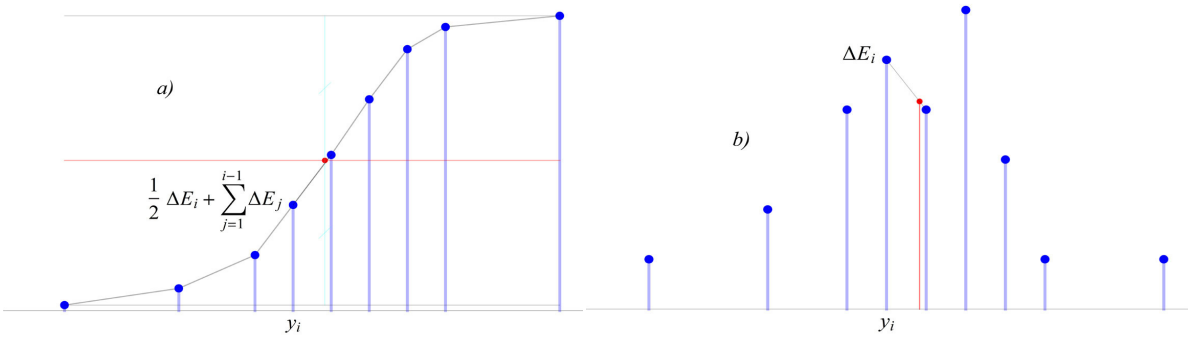

Fig. 2. The calculation of location and energy weight for median of the energy release distribution in silicon-strip layer. The distribution of the sum of energy releases in strips along strip positions (a), the estimation of median energy location in silicon-strip layer (b).

To find the energy weight of the median the ordinary distribution of energy releases in strips along strip positions is built (Fig. 2b). The median energy weight is defined using the obtained median location for the piece line linking adjacent (respective median location) points of the obtained distribution (Fig. 2b). Then the estimation of the initial direction is obtained using fitting procedure for the median locations in silicon-strip layers. Around the estimated direction the corridor from strips is constructed. The energy releases in strips outside the corridor are ignored. After

that the iteration procedure starts, narrowing the corridor from strips in each silicon-strip layer, but not less, then five strip pitch. For each iteration step the median energy weight from previous iteration is taken into account.

To calculate the angular resolution, the distribution of a space angular deflection between the direction reconstructed for each event and the median value for all events in distribution is analyzed. Such distribution for 100 GeV gamma-quanta is shown in Fig. 3. Angular resolution is defined a semiopening of the circular conical surface, containing 68% of events. The computed angular resolution calculated using this value is shown in Fig. 4. as function of initial energy for incident and polar angle of gamma equal 5^0. The results are not changing significantly at least for incident angles till 15^0. The FERMI experiment data [6] for front section are also shown in Fig. 4. For the energies more than 10 GeV the GAMMA-400 gamma-ray telescope provides several times better angular resolution.

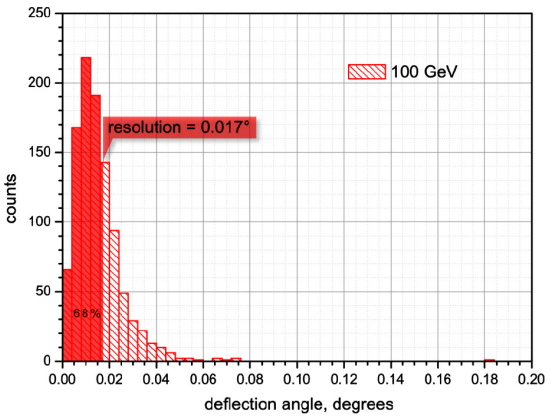

Fig. 3. The distribution of space angular deflections between the reconstructed direction of each event and the median value of the total distribution.

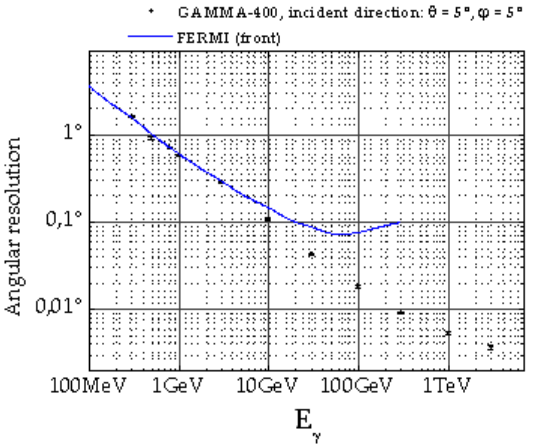

Fig. 4. The energy dependence of GAMMA-400 angular resolution.

4. Methods to reject protons from electrons using the GAMMA-400 gamma-ray telescope systems during ground data processing

The methods to reject protons from electrons were processed with the GEANT4 simulation toolkit software [5]. Protons produce the main background, when detecting cosmic-ray electrons, since a fraction of the lepton component is $\sim 10^{-3}$ of the total cosmic-ray flux for high energies. For charged particles and gamma rays onboard identification the signals from AC detectors are used in the trigger system due specially designed for GAMMA-400 methods of backsplash rejection. In addition, the information from ND, S4, S3, S2, CC1, and CC2 detectors is used during ground data processing for rejection protons from electrons due algorithm discussed in the article presented.

Proton rejection factor should take into account the final proton contamination in the resulting reconstructed electron flux. It could be calculated by applying the electron selections separately to the proton and the electron spectra and by constructing energy histogram with surviving electrons and protons in each energy bin. This will immediately provide the electron detection efficiency, which can be transferred in the effective geometric factor for electrons, and proton contamination. After that, in order to calculate the flux, it is necessary just simply to multiply the total flux (electrons + residual protons) by the simulated value.

In principle, any of protons with energy more than 100 GeV could imitate 100 GeV electrons (with different probabilities, of course). The set of the detectors: S2, S4, S3, CC1, CC2, and S4 is considered as separate layers of composite calorimeter, and the ability of each layer is investigated separately to decrease the proton contamination in the different energy bins of electrons. The rejection factor to separate protons from electrons with energy 100 GeV is calculated as the ratio of the number of initial protons with energy more than 100 GeV, assuming that the proton energy spectrum power is -2.7, to the number of events identified as electrons with energy 100±2 GeV (taking into account that the GAMMA-400 energy resolution is equal to about 2%). This approach is specific for the

instrument configuration, taking into account the total depth of the matter (~1/2 λ_0), which defines the probability of proton nuclear interactions inside the calorimeter, the mean energy of protons that might mimic 100 GeV electrons, and the energy resolution. The intrinsic rejection power of GAMMA-400 just due to its interaction depth and energy resolution is implicitly contributed in the analyses for each layer of composite calorimeter.

Taking into account the GAMMA-400 instrument structure, the information from CC2 can be applied for rejection using lateral distribution of particles in the calorimeter; S4 responses allow us to reduce proton contamination from the longitudinal shower development. The initial point of the shower is utilized from the information of S2, S3, and CC1 detectors. The information from neutron detector also essentially improves separation of electrons from protons, especially for the energy more, than 50 GeV [4].

In this paper the contamination for vertical incident protons is evaluated. All processed criteria to suppress protons are based on selecting cutoffs to distinguish proton and electron events. The location of the cutoff for each criterion is selected in order to retain 98% of electrons. Totally 25 cutoffs are used to reject protons. Taking into account presented selection ~30% of electrons are also lost due to proton rejection. The description of the criteria is ordered according to their own rejection power, excepting the number of neutrons in ND. Because the ND efficiency in view of neutrons detection will be the purpose of the next more detailed calculations, the power of the ND criterion can be considered as upper estimation of own rejection. This is not critical due to the fact that the refusal of this criterion does not reduce the total rejection more than 2 times.

The information from S4 provides the strongest own rejection factor for protons. This rejection concerns with the difference in the attenuation for hadronic and electromagnetic cascades. Electromagnetic shower initiated by the electron with initial energy of ~ 100 GeV is fully contained inside the calorimeter with the thickness 25 X_0 or 1.2 λ_0. Such criterion was used in the PAMELA experiment data analysis [7].

The distributions for signals in S4 from initial electrons and protons are shown in Figs. 5a and 5c. Selecting events with signals in S4 less than 2.7 MIP, it is possible to suppress protons with a factor of 100.

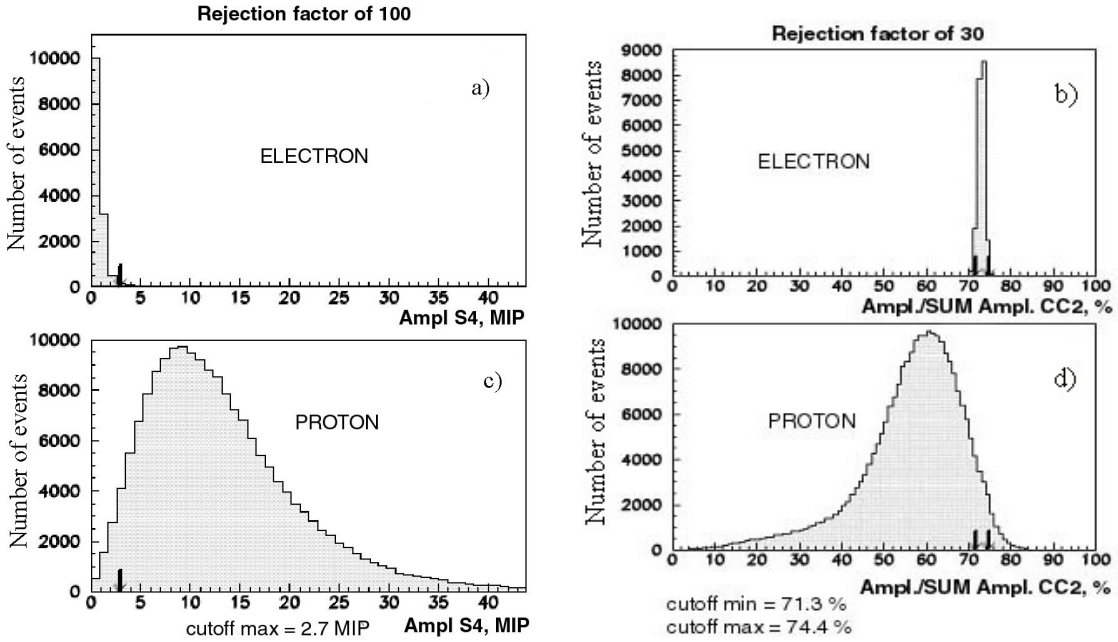

Fig. 5. The distributions for signals in S4 from initial electrons (a) and protons (c). The distributions for the ratio of a signal in the crystal containing the cascade axis to the value of total signal in CC2 for initial electrons (b) and protons (d).

Additional rejection is obtained when analyzing total CC2 signals. The CC2 calorimeter contains CsI(Tl) square crystals with cross dimension of 36 mm and longitudinal dimension of 430 mm. The criterion is based on the difference of the transversal size for hadronic and electromagnetic showers. Such topology difference was

successfully applied with the calorimeter data in the PAMELA mission to separate electrons from antiproton sample and positrons from proton sample [7, 8]. The distributions for the ratio of a signal in the crystal containing cascade axis to the value of total signal in CC2 for initial electrons and protons are compared (Figs 5b and 5d). Using the distribution for the initial electrons, the values of two cutoffs are determined as 71.3% and 74.4%. For the proton distribution, only events placed between these electron cutoffs are retained. Applying this rejection provides the rejection factor of ~30.

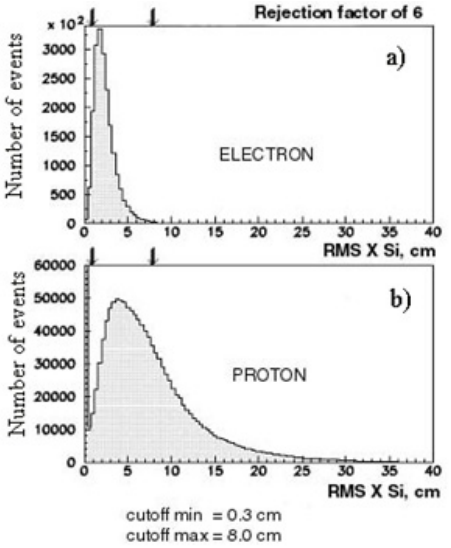

Fig. 6. The distribution for RMS of coordinates of strips with signals in CC1 for initial electrons (a) and protons (b).

The differences in proton and electron cascade transversal size are also used when analyzing information from silicon strips in CC1. The distributions for RMS of coordinates of strips with signals for initial electrons and protons are shown in Figs. 6a and 6b. For the proton distribution, only events placed between the cutoffs of 0.3 cm and 8 cm obtained from the electron distribution are retained. Applying this rejection provides the rejection factor of ~6.

To take into account the fact that the hadronic cascade begins to develop deeper inside the instrument, than the electromagnetic shower, the signals in detector systems CC1 (crystal), S2 and S3 are considered, using the fact that the thickness of material just above these detectors is less than 4 X_0. The distributions of signals in second layer of crystal CsI(Tl) from CC1 and of signals in S3 from initial electrons and protons are shown in Fig. 7. For proton-induced cascades, there are a lot of events with small signal amplitude. To reject such events the cutoff from electron induced cascades distribution is determined. The events from proton induced distribution with the value of signal less than this cutoff are rejected. This criterion allows us to suppress protons with the factor of 3 for each CsI(Tl) crystal from CC1 and with the factor of 2 for each scintillation detector S2 and S3.

Table 1. Own rejection factor for protons of each detector system (without other) and the values of total rejection factor decreasing in the case of the refusal of given rejection.

Detector system, number of cutoffs	Own rejection factor	Total rejection factor decreasing
S4 (2 cutoffs: 1 cutoff for each scintillation layer)	100	1.7
CC2 (2 cutoffs)	30	2.6
Strips in CC1 (4 cutoffs: 2 cutoffs for each X or Y silicon strip)	6	1.2
CsI(Tl) from CC1 (2 cutoffs: 1 cutoff for each layer of CsI(Tl) crystal)	3	1.3
S2, S3 (4 cutoffs: 2 cutoffs for each detector)	2	1.3
ND (1 cutoff)	400 (upper limit)	2

The ND contribution in the rejection factor for protons in the GAMMA-400 telescope is considered with significantly different number of neutrons generated in the electromagnetic and hadronic cascades. In cascades, induced by protons, the generation of neutrons is more intensive than in the electromagnetic shower. The source of neutrons in cascades, induced by electrons, concerns mainly with generation of gamma rays in those cascades with energy close to 17 MeV. These gamma rays, in turn, could generate neutrons in the Giant resonance reaction. Analyzing information from the neutron detector placed just under the CC2 calorimeter, it is possible to suppress protons by the factor of 400. The distributions for number of neutrons at the entrance of ND from initial electrons and protons are shown in Fig. 8. The cutoff for the number of neutrons to separate protons is equal to 60. The efficiency of neutron detection is not taken into account in the present simulation, but will be the purpose of the next more detailed calculations. The power of this criterion can be considered as upper estimation of own rejection.

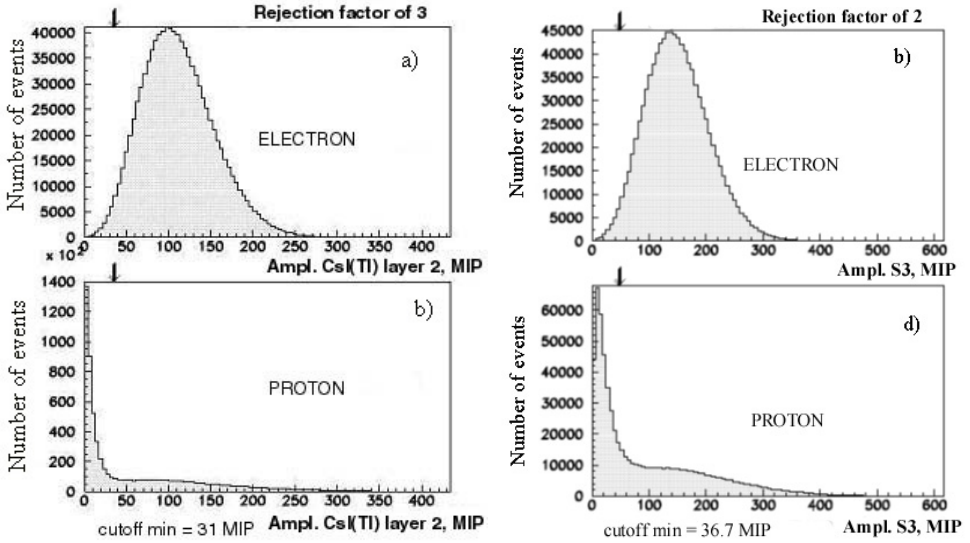

Fig. 7. The distributions of signals in second crystal CsI(Tl) of CC1 from initial electrons (a) and protons (c). The distributions of signals in S3 from initial electrons (b) and protons (d).

All above discussed proton rejection criteria were considered separately from each other. Using all criteria in the combination, it is possible to obtain rejection factor for protons equal to $(4\pm0.4)\times10^5$. Table 1 contains the information about own rejection factor of each criterion (without other) and the values of the total rejection factor decreasing in the case of the refusal from given criterion. All of presented criteria are strongly dependent that is confirmed by the values in the right column. The refusal from any given criterion, especially the strongest from S4, CC2, and CC1 detectors, reduces the total rejection factor significantly less than dividing with own rejection number of this criterion.

The same calculations were performed for the energy range from 50 GeV to 1 TeV. Table 2 contains the information concerning the rejection factor to separate protons from electrons in this energy range.

Table 2.Total rejection factor to separate protons from electrons in energy range from 50 GeV to 1 TeV.

Energy, GeV	Total rejection factor
50	$(12.8\pm2.0)\times10^5$
10^2	$(4.0\pm0.4)\times10^5$
2×10^2	$(5.0\pm0.7)\times10^5$
10^3	$(4.1\pm0.7)\times10^5$

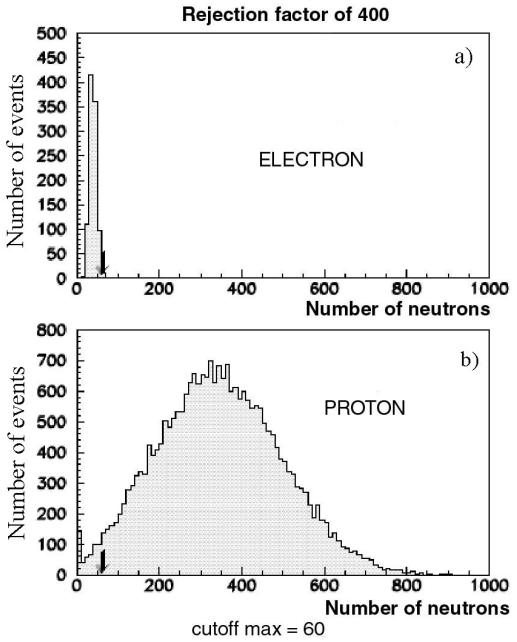

Fig. 8. The distributions of the number of neutrons at the entrance of ND for electrons (a) and protons (b).

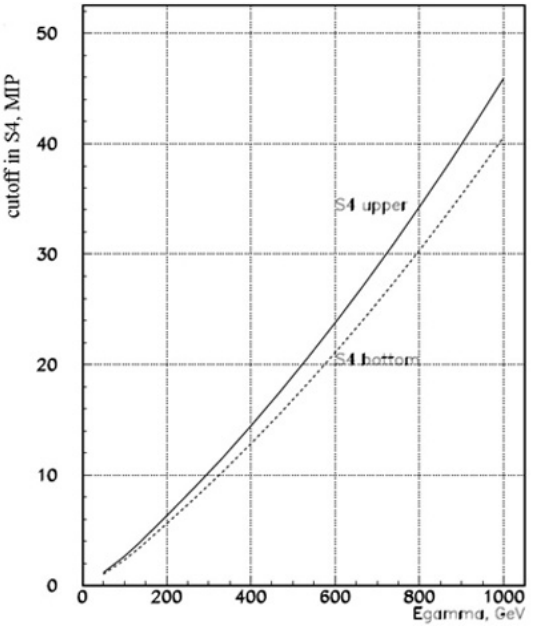

Fig. 9. The dependence of the cutoffs in upper (solid line) and bottom (dotted line) layers of the S4 detector versus the gamma-ray initial energy.

The absolute values of all described cutoffs are increased with the gamma-ray initial energy. As an example, the dependence of the cutoffs in upper and bottom layers of the S4 detector versus the gamma-ray initial energy is presented in Fig. 9. The value of the cutoff in MIPs for the each energy is selected in order to retain 98% of electrons (Figs. 5a and 5c).

5. Conclusion

The processed methods allow us to reconstruct the direction of electromagnetic shower axis. As a result, the direction of incident gamma-quanta with the energy of 100 GeV is calculated with an accuracy of better than 0.02 deg.

Using the combined information from all detector systems of the GAMMA-400 gamma-ray telescope, it is possible to provide effective rejection of protons from electrons. The proposed methods are based on the difference of the development of hadronic and electromagnetic showers inside the instrument. It was shown that the rejection factor for protons is several times better than 10^5. Such kind of separation extends in the energy range from 50 GeV to 1 TeV.

References

[1]Galper A.M., Adriani O., Aptekar R.L. *et al.* Status of the GAMMA-400 project. *Adv. Space Res.* 2013;51:297–300.

[2]Fabjan C.W. and Gianotti F. Calorimetry for particle physics, *Rev. Mod. Phys.* 2003;75:1243-1286, CERN-EP-2003-075.

[3]Adriani O., Barbarino G.C., Bazilevskaya G.A. *et al.* An anomalous positron abundance in cosmic rays with energies 1.5–100 GeV, *Nature, Letters*. 2009;458(2):607-609.

[4]Stozhkov Y.I., Basili A., Bencardino R. *et al.* About separation of hadron and electromagnetic cascades in the PAMELA calorimeter, *International Journal of Modern Physics A*. 2005;20(29):6745–6748.

[5]*http://geant4.cern.ch*

[6]*http://www.slac.stanford.edu/exp/glast/groups/canda/ lat_Performance.htm*

[7]Karelin A.V., Borisov S. V., Voronov S. A. *et al.* Separation of the electron and proton cosmic-ray components by means of a calorimeter in the PAMELA satellite-borne experiment for the case of particle detection within a large aperture, *Physics of Atomic Nuclei*. 2013;76(6):737–747.

[8]Menn, W., Adriani, O., Barbarino, G.C. *et al.* The PAMELA space experiment, *Adv. Space Res.* 2013;51:209–218.